HHS Public Access

Author manuscript

Nature. Author manuscript; available in PMC 2011 January 01.

Published in final edited form as:

Nature. 2010 July 29; 466(7306): 632–636. doi:10.1038/nature09173.

Cross-species genomics matches driver mutations and cell compartments to model ependymoma

Robert A. Johnson[1,*], **Karen D. Wright**[1,12,*], **Helen Poppleton**[1], **Kumarasamypet M. Mohankumar**[1], **David Finkelstein**[2], **Stanley B. Pounds**[3], **Vikki Rand**[4], **Sarah E.S. Leary**[5], **Elsie White**[1], **Christopher Eden**[1], **Twala Hogg**[1], **Paul Northcott**[6], **Stephen Mack**[6], **Geoffrey Neale**[2], **Yong-Dong Wang**[2], **Beth Coyle**[7], **Jennifer Atkinson**[1], **Mariko DeWire**[12], **Tanya A. Kranenburg**[1], **Yancey Gillespie**[8], **Jeffrey C. Allen**[9], **Thomas Merchant**[10], **Fredrick A. Boop**[11], **Robert. A. Sanford**[11], **Amar Gajjar**[12], **David W. Ellison**[13], **Michael D. Taylor**[6], **Richard G. Grundy**[7], and **Richard J. Gilbertson**[1,12]

[1]Dept. of Developmental Neurobiology, St Jude Children's Research Hospital, 262 Danny Thomas Place, Memphis, TN, 38105, USA

[2]Dept. of Hartwell Centre for Bioinformatics and Biotechnology, St Jude Children's Research Hospital, 262 Danny Thomas Place, Memphis, TN, 38105, USA

[3]Dept. of Biostatistics, St Jude Children's Research Hospital, 262 Danny Thomas Place, Memphis, TN, 38105, USA

[4]Northern Institute for Cancer Research, University of Newcastle upon Tyne, Newcastle upon Tyne, UK

[5]Hematology-Oncology, Seattle Children's Hospital, Seattle, WA 98105, USA

[6]Division of Neurosurgery, Arthur and Sonia Labatt Brain Tumour Research Centre, Hospital for Sick Children, Toronto, Ontario, Canada

[7]Children's Brain Tumor Research Centre, University of Nottingham, Nottingham, UK

[8]Dept. Surgery 1900 University Boulevard, Birmingham, AL 35294

[9]NYU Langone Medical Center, 550 First Avenue, New York, NY 10016

[10]Dept. of Radiological Sciences, St Jude Children's Research Hospital, 262 Danny Thomas Place, Memphis, TN, 38105, USA

Correspondence should be addressed to RJG: Richard.Gilbertson@stjude.org.

*These authors contributed equally to this study.

Author Contributions. R. Gilbertson, R. Grundy, and M. Taylor, conceived the research and planned experiments. R. Johnson and K. Wright, also planned and conducted the great majority of the experiments under the direction of R. Gilbertson. A. Gajjar, Y. Gillespie, J. Allen, M. Taylor, and R. Grundy, provided human tumor material. All authors contributed experimental expertise and participated in the writing of the manuscript. D. Finklestein, S. Pounds, Y-D. Wang and G. Neale, provided bioinformatic expertise. D. Ellison. provided pathology review and iFISH analysis.

Supplementary Information

Supplemental Information is available online.

Competing interests

None

[11]Dept. of Surgery, St Jude Children's Research Hospital, 262 Danny Thomas Place, Memphis, TN, 38105, USA

[12]Dept. of Oncology St Jude Children's Research Hospital, 262 Danny Thomas Place, Memphis, TN, 38105, USA

[13]Dept. of Pathology, St Jude Children's Research Hospital, 262 Danny Thomas Place, Memphis, TN, 38105, USA

Abstract

Understanding the biology that underlies histologically similar but molecularly distinct subgroups of cancer has proven difficult since their defining genetic alterations are often numerous, and the cellular origins of most cancers remain unknown1–3. We sought to decipher this heterogeneity by integrating matched genetic alterations and candidate cells of origin to generate accurate disease models. First, we identified subgroups of human ependymoma, a form of neural tumor that arises throughout the central nervous system (CNS). Subgroup specific alterations included amplifications and homozygous deletions of genes not yet implicated in ependymoma. To select cellular compartments most likely to give rise to subgroups of ependymoma, we matched the transcriptomes of human tumors to those of mouse neural stem cells (NSCs), isolated from different regions of the CNS at different developmental stages, with an intact or deleted *Ink4a/Arf* locus. The transcriptome of human cerebral ependymomas with amplified *EPHB2* and deleted *INK4A/ARF* matched only that of embryonic cerebral *Ink4a/Arf*$^{-/-}$ NSCs. Remarkably, activation of Ephb2 signaling in these, but not other NSCs, generated the first mouse model of ependymoma, which is highly penetrant and accurately models the histology and transcriptome of one subgroup of human cerebral tumor. Further comparative analysis of matched mouse and human tumors revealed selective deregulation in the expression and copy number of genes that control synaptogenesis, pinpointing disruption of this pathway as a critical event in the production of this ependymoma subgroup. Our data demonstrate the power of cross-species genomics to meticulously match subgroup specific driver mutations with cellular compartments to model and interrogate cancer subgroups.

Ependymomas are tumors of the brain and spinal cord4. Surgery and irradiation remains the mainstay of treatment of this disease since chemotherapy is ineffective in most patients. Consequently, ependymoma is incurable in up to 40% of cases5. Despite histologic similarities, ependymomas from different regions of the CNS display disparate prognoses, transcriptional profiles and genetic alterations6–8, suggesting they are different diseases and confounding efforts to study, model and treat these tumors.

To understand the biological basis of ependymoma heterogeneity, we catalogued DNA copy number alterations (CNAs) among 204 tumor samples and generated messenger (m)RNA and micro (mi)RNA expression profiles for 83 and 64 of these tumors, respectively (Supplemental Figure 1, Supplemental Table 1). mRNA profiles segregated tumors by CNS location and unmasked previously unknown subgroups among supratentorial, posterior fossa and spinal ependymomas (Subgroups A to I, Figure 1). Notably, miRNAs segregated tumors by location and subgroup in a manner that significantly matched that of mRNA profiles (Rand index for mRNA subgroup match=0.88, P<0.0001;Supplemental Figure 2). Large

chromosomal CNAs occurred most frequently in spinal tumors, enriching their mRNA expression signature for genes gained and over-expressed on chromosomes 4, 7, 9, 12, 15q and 18q and deleted and under-expressed on 22q (permutation analysis of each, P<0.005; Supplemental Figures 3 and 4; Supplemental Table 2a). Similarly, deletion and under-expression of chromosomes 3, 9 and 22q enriched the expression signature of subgroup C, while deletion and under-expression of 6q was observed in subgroup H (Supplemental Figure 4). The observation that mRNA, miRNA and CNA profiles cluster ependymomas into similar subgroups supports the notion that these subgroups are true biologic entities.

In addition to large chromosomal alterations we identified 175 focal amplifications (average size 159kb) and 157 focal deletions (average size 199kb) encoding 1,236 and 1,209 transcripts, respectively (see Supplemental Methods section, Supplemental Table 3 and Supplemental Gene Cards). In contrast to large alterations, focal CNAs occurred most frequently in supratentorial ependymomas (Supplemental Table 2b). Alignment of each focal CNA against the database of Copy Number Variants (CNVs) revealed which overlapped with known CNVs (http://projects.tcag.ca/variation/), but these were not excluded from further analysis since recent data suggests CNVs might contribute to disease states including cancer9. Fifty-one of 57 selected CNAs that were likely to encode oncogenes or tumor suppressor genes (TSGs) were validated by Real-Time PCR and/or fluorescence *in situ* hybridization (FISH) (Figure 1; Supplemental Table 4; Supplemental Gene Cards; see Supplemental Methods for selection criteria). This extensive analysis confirmed and refined previously reported CNAs (e.g., deletion of *INK4A/ARF*7, amplification of *NOTCH1*8, and three discrete focal 22q deletions), and identified 28 and 23 novel recurrent focal amplifications and deletions, respectively.

To prioritize for further study genes within focal CNAs that may have driven clonal selection, we correlated DNA copy number with the level of transcripts encoded by each affected loci (Supplemental Gene Cards). Seventeen percent (n=107/632) of genes located within 28 validated focal amplicons displayed evidence of copy number driven expression, highlighting them as potential ependymoma oncogenes (Supplemental Table 5a). Notably, these included several regulators of stem cell proliferation, pluripotency and neural differentiation e.g., *THAP11*10, *PSPH*11, *EPHB2*12, ten genes within the *PCDH* cluster13, *KCNN1*14, *RAB3A*15,16, *PTPRN2*17 and *NOTCH1*18, the latter being the only candidate ependymoma oncogene identified to date8. Eighteen-percent (n=130/728) of genes located within 23 validated focal deletions displayed copy number driven decreased expression compatible with these being TSGs (Supplemental Table 5b and Supplemental Gene Cards). These included established TSGs previously implicated in ependymoma7 e.g., *PTEN*, *CDKN2A/CDKN2B*, as well as genes with no prior known role in cancer (e.g., *STAG1* [3q22.3] and *TNRC6B* [22q13.1]). Since the few known candidate ependymoma oncogenes and TSGs were identified by our comprehensive bioinformatics, we suggest that the other genes identified here are highly enriched for those involved in ependymoma tumorigenesis.

Recently, we showed that intracranial and spinal ependymomas are propagated by radial glia (RG)-like cancer stem cells7. RG function as NSCs in the embryo and give rise to adult NSCs19,20. Throughout development NSCs located in the different regions of the CNS display intrinsic biological differences that include the expression of variable transcription

factor profiles and the production of different kinds of neurons19,21. Therefore, we reasoned that individual subgroups of ependymoma might arise from regionally and developmentally distinct NSCs that are susceptible to transformation by different gene mutations. To test this hypothesis we first established a robust source of RG (hereon, embryonic NSCs) and adult NSCs. Enhanced green fluorescent protein (eGFP)$^+$ cells were isolated from the cerebrum, hindbrain and spine of embryonic day (E) 14.5 and adult *Blbp-eGFP* transgenic mice that express eGFP within the embryonic NSC-astroglial-adult NSC lineage22–24 (Figure 2). eGFP$^+$ cells were isolated from both *Ink4a/Arf*$^{+/+}$ and *Ink4a/Arf*$^{-/-}$ mice since this locus is frequently deleted from human cerebral ependymomas (Figure 1; Supplemental Gene Cards). When cultured under conditions that promote stem cell growth, all 12 distinct eGFP$^+$ cell isolates were demonstrated to be NSCs that displayed a Nestin$^+$/Prom1$^+$/Gfap$^+$/Rc2$^+$/Blbp$^+$ immunophenotype19 and self-renewed as clonal multipotent neurospheres (Figure 2a and b; Supplemental Figure 5). mRNA expression profiles of 177 separate NSC cultures segregated these cells according to location (intracranial vs. spine) and developmental stage (embryonic vs. adult), and further segregated adult intracranial NSCs by brain region (cerebral vs. hindbrain) and *Ink4a/Arf* status (Figure 2b). Notably, cerebral and hindbrain NSCs isolated from *Ink4a/Arf*$^{-/-}$ adult mice displayed an increased self-renewal capacity (Figure 2b). Together, these data confirm functional differences between regionally, developmentally and genetically defined NSC isolates and validate reports that increasing Cdkn2a expression negatively regulates self-renewal in aging cerebral NSCs25.

To pinpoint which NSCs might give rise to ependymoma subgroups, we developed a novel algorithm that we termed *ag*reement of *d*ifferential *ex*pression (AGDEX) that detects transcriptomic similarities between tissues from different species by comparing the expression of shared orthologs (see Supplemental Methods). The transcriptome of cerebral ependymomas significantly matched only that of embryonic cerebral *Ink4a/Arf*$^{-/-}$ NSCs (n=14,261 orthologs, permuted $P<0.05$). Conversely, spinal ependymomas were most similar to adult spinal NSCs (permuted $P<0.005$). Interestingly, these development-dependent correlations reflect the epidemiology of the disease: cerebral ependymomas affect three times more pediatric than adult patients, while spinal ependymomas are five times more common in adults26. These data pinpoint embryonic cerebral NSCs and adult spinal NSCs as putative cells of origin of cerebral and spinal ependymoma, respectively, and support genetic evidence that deletion of *INK4A/ARF* is important in the development of cerebral ependymoma.

To test directly if embryonic cerebral *Ink4a/Arf*$^{-/-}$ NSCs represent a specific source of cerebral ependymomas, we challenged these cells with Ephb2 that we identified to be selectively amplified and/or over-expressed in these tumors (Figure 3a and b) and that was shown recently to regulate stem cell proliferation and tumorigenesis in the intestine27. For comparative purposes, we also challenged a panel of four other NSC isolates (Figure 3c and d). Freshly isolated eGFP$^+$ NSCs were transduced at second neurosphere passage with *Ephb2*-Red Fluorescence Protein (*EphB2*^{RFP}) or control (cRFP) viruses (Figure 3c). 1×10^6 eGFP$^+$/RFP$^+$ NSCs were then implanted in the cerebrum of immunocompromised mice which were observed for signs of tumor development. None of 120 mice implanted with

control-transduced NSCs developed tumors (median follow up 227 days, Figure 3d). Mice implanted with *Ephb2*^{RFP} transduced embryonic cerebral *Ink4a/Arf*$^{+/+}$, adult cerebral *Ink4a/Arf*$^{-/-}$, embryonic hindbrain *Ink4a/Arf*$^{-/-}$ or adult spinal *Ink4a/Arf*$^{-/-}$ NSCs developed tumors with non-ependymal histologies at very low rates (9.6%, n=9/94 median follow up 241 days; Figure 3d; Supplemental Figure 6). In stark contrast, 50% of mice implanted with *Ephb2*^{RFP} transduced embryonic cerebral *Ink4a/Arf*$^{-/-}$ NSCs developed EphB2^{+}/eGFP^{+}/RFP^{+} brain tumors within 200 days of implantation, and less than 30% were tumor-free by 300 days (Log Rank P<0.0005, median follow up 230 days, Figure 3d). Remarkably, these mouse tumors were histologically indistinguishable from human ependymomas, displaying characteristic pseudo-rosettes, a uniform (non-nodular) distribution of cells and clear cell phenotype—all hallmarks of certain cerebral ependymomas (Figure 4a)28. Furthermore, electron microscopy identified microvilli, cilia and tight junctions in these mouse tumors that are classic ultrastructural features of human ependymoma (Figure 4b). Thus, the specific combination of embryonic cerebral NSCs, deletion of *Ink4a/Arf* and amplification of *EphB2* generates cerebral ependymoma, supporting strongly the hypothesis that ependymoma variants arise from specific combinations of susceptible NSCs and matched mutations.

To test further the fidelity of this new mouse model of cerebral ependymoma, we used the AGDEX algorithm to correlate the ortholog expression profiles of 12 *Ephb2*-driven mouse ependymomas with those of human ependymoma subgroups (A to I) as well as previously described molecular subgroups of human glioblastoma29 and medulloblastoma30. This analysis confirmed a highly significant and selective match between mouse and human cerebral ependymoma but no other tested human brain tumor (permuted P <0.0001, Figure 4c). Remarkably, the transcriptome of our mouse model matched a single human cerebral ependymoma subgroup (D), validating subgroup D as a true disease entity. Review of the orthologs that were most significantly and differentially expressed in both *Ephb2*-driven mouse ependymomas (relative to embryonic cerebral *Ink4a/Arf*$^{-/-}$ NSCs) and human subgroup D tumors (relative to other human tumors) revealed these to be highly enriched for regulators of neural differentiation and maintenance, particularly ion transport and synaptogenesis (n=70/160, Fisher's Exact Test, Q<0.0001, Supplemental Table 6). Eleven of these common signature orthologs were also targeted by CNAs in subgroup D tumors, of which six directly regulate neurogenesis and maintenance (Supplemental Table 6). Thus, we predict that aberrant EPHB2 signaling and deletion of *INK4A/ARF* disrupts key neural differentiation pathways in embryonic cerebral NSCs during the formation of subgroup D ependymoma.

We describe a novel cross-species genomic approach that meticulously matches subgroup specific driver mutations and appropriate cellular compartments to model human cancer subgroups. Similar efforts are underway to model and validate the remaining human ependymoma subgroups. The approach described here could be applied to other cancers, enabling the identification and matching of candidate cells of origin with appropriate mutations to decipher molecular subgroups.

Methods Summary

Tissue samples and genomics

Human ependymoma samples were obtained from tumor banks with Institutional Review Board approval. Human and mouse tumors comprised a minimum of 85% tumor cells. Expression profiles were generated using Affymetrix U133 Plusv2 (mRNA human) and 430v2 (mRNA mouse) arrays and Agilent miRNA arrays (human). Expression profiles of 53 human medulloblastomas and 76 glioblastomas were obtained from previously published studies29,30. DNA copy number analyses were performed using the Affymetrix 500K SNP mapping arrays. CNAs were validated by real-time PCR (see Supplemental Table 4) and/or FISH as appropriate7. mRNA and miRNA expression profiles and DNA CNAs were analyzed, validated and integrated using established and novel bioinformatic and statistical approaches (see Supplemental Methods). Common orthologs were filtered from human mouse mRNA expression arrays using sequence mapping.

NSC cultures and implants

Blbp-eGFP transgenic mice were the generous gift of Dr. Nathaniel Heintz (Rockefeller University), FVB.129-*Cdkn2a*^{tm1Rdp} mice were from the MMHCC repository. eGFP^{+} cells were isolated from *Blbp-eGFP* mouse brains and spines and cultured in neural stem cell medium as described7. NSCs were transduced with RFP-retroviruses and eGFP^{+}/RFP^{+} cells sorted using a Becton Dickinson Aria II Cell Sorter. Clonal neurosphere formation and differentiation capacities were assessed in serial dilutions of single-cell suspensions7. NSCs were implanted under stereotactic control into the forebrain of immunocompromised mice and animals were observed daily for signs of tumor development7. All mouse brains were inspected by macroscopic dissection post-mortem. Fresh tumor cells were recovered from mouse brains as described7.

Histology

Sections of human and mouse ependymomas were prepared from formalin paraffin embedded tissues. Protein expression was detected in formalin fixed tissue sections and differentiated NSCs using standard immunohistochemical and immunofluorescence techniques. Electron microscopy was performed using standard tissue preparations and a FEI Tecnai 20 200KV FEG Electron Microscope. Western blot analysis was used to detect protein expression in fresh tissue and cells (for antibodies see Supplemental Methods).

Supplementary Material

Refer to Web version on PubMed Central for supplementary material.

Acknowledgements

R.J.G. holds the Howard C. Schott Research Chair from the Malia's Cord Foundation, and is supported by grants from the National Institutes of Health (R01CA129541, P01CA96832 and P30CA021765), the Collaborative Ependymoma Research Network (CERN) and by the American Lebanese Syrian Associated Charities (ALSAC). K.D.W. is supported by NRSA Training Grant T32 CA070089. We are grateful to the Dr. Nathaniel Heintz for providing the *Blbp-eGFP* mouse, Dr. Tony Pawson for providing mouse Ephb2 cDNA, Dr. Martine Roussel for the PCX4-IRES-RFP virus, Drs. Downing and Relling for access to 500K SNP profiles of normal human DNA, and the

staff of the Hartwell center for Bioinformatics and Biotechnology, Vector Production Core, ARC, AIC and Cell and Tissue Imaging at St Jude Children's Research Hospital for technical assistance.

References

1. Parsons DW, et al. An integrated genomic analysis of human glioblastoma multiforme. Science. 2008; 321:1807–1812. [PubMed: 18772396]
2. Stommel JM, et al. Coactivation of receptor tyrosine kinases affects the response of tumor cells to targeted therapies. Science. 2007; 318:287–290. [PubMed: 17872411]
3. TCGA Comprehensive genomic characterization defines human glioblastoma genes and core pathways. Nature. 2008; 455:1061–1068. [PubMed: 18772890]
4. Kleihues P, et al. The WHO classification of tumors of the nervous system. J Neuropathol Exp Neurol. 2002; 61:215–225. discussion 226-219. [PubMed: 11895036]
5. Merchant TE, et al. Conformal radiotherapy after surgery for paediatric ependymoma: a prospective study. Lancet Oncol. 2009; 10:258–266. [PubMed: 19274783]
6. Modena P, et al. Identification of tumor-specific molecular signatures in intracranial ependymoma and association with clinical characteristics. J Clin Oncol. 2006; 24:5223–5233. [PubMed: 17114655]
7. Taylor MD, et al. Radial glia cells are candidate stem cells of ependymoma. Cancer Cell. 2005; 8:323–335. [PubMed: 16226707]
8. Puget S, et al. Candidate genes on chromosome 9q33-34 involved in the progression of childhood ependymomas. J Clin Oncol. 2009; 27:1884–1892. [PubMed: 19289631]
9. Diskin SJ, et al. Copy number variation at 1q21.1 associated with neuroblastoma. Nature. 2009; 459:987–991. [PubMed: 19536264]
10. Dejosez M, et al. Ronin is essential for embryogenesis and the pluripotency of mouse embryonic stem cells. Cell. 2008; 133:1162–1174. [PubMed: 18585351]
11. Nakano I, et al. Phosphoserine phosphatase is expressed in the neural stem cell niche and regulates neural stem and progenitor cell proliferation. Stem Cells. 2007; 25:1975–1984. [PubMed: 17495110]
12. Kayser MS, Nolt MJ, Dalva MB. EphB receptors couple dendritic filopodia motility to synapse formation. Neuron. 2008; 59:56–69. [PubMed: 18614029]
13. Chess A. Monoallelic expression of protocadherin genes. Nat Genet. 2005; 37:120–121. [PubMed: 15678142]
14. Cueni L, et al. T-type Ca2+ channels, SK2 channels and SERCAs gate sleep-related oscillations in thalamic dendrites. Nat Neurosci. 2008; 11:683–692. [PubMed: 18488023]
15. Gogolla N, et al. Wnt signaling mediates experience-related regulation of synapse numbers and mossy fiber connectivities in the adult hippocampus. Neuron. 2009; 62:510–525. [PubMed: 19477153]
16. Geppert M, et al. The small GTP-binding protein Rab3A regulates a late step in synaptic vesicle fusion. Nature. 1997; 387:810–814. [PubMed: 9194562]
17. Taraska JW, Almers W. Bilayers merge even when exocytosis is transient. Proc Natl Acad Sci U S A. 2004; 101:8780–8785. [PubMed: 15173592]
18. Dahlhaus M, et al. Notch1 signaling in pyramidal neurons regulates synaptic connectivity and experience-dependent modifications of acuity in the visual cortex. J Neurosci. 2008; 28:10794–10802. [PubMed: 18945887]
19. Kriegstein A, Alvarez-Buylla A. The Glial Nature of Embryonic and Adult Neural Stem Cells. Annu Rev Neurosci. 2009; 32:149–184. [PubMed: 19555289]
20. Merkle FT, et al. Radial glia give rise to adult neural stem cells in the subventricular zone. Proc Natl Acad Sci U S A. 2004; 101:17528–17532. Epub 12004 Dec 17521. [PubMed: 15574494]
21. Kriegstein AR, Gotz M. Radial glia diversity: a matter of cell fate. Glia. 2003; 43:37–43. [PubMed: 12761864]
22. Anthony TE, et al. Brain lipid-binding protein is a direct target of Notch signaling in radial glial cells. Genes Dev. 2005; 19:1028–1033. [PubMed: 15879553]

23. Gong S, et al. A gene expression atlas of the central nervous system based on bacterial artificial chromosomes. Nature. 2003; 425:917. [PubMed: 14586460]
24. Schmid RS, Yokota Y, Anton ES. Generation and characterization of brain lipid-binding protein promoter-based transgenic mouse models for the study of radial glia. Glia. 2006; 53:345–351. [PubMed: 16288463]
25. Molofsky AV, et al. Increasing p16INK4a expression decreases forebrain progenitors and neurogenesis during ageing. Nature. 2006; 443:448–452. [PubMed: 16957738]
26. McGuire CS, Sainani KL, Fisher PG. Incidence patterns for ependymoma: a surveillance, epidemiology, and end results study. J Neurosurg. 2009; 110:725–729. [PubMed: 19061350]
27. Genander M, et al. Dissociation of EphB2 signaling pathways mediating progenitor cell proliferation and tumor suppression. Cell. 2009; 139:679–692. [PubMed: 19914164]
28. Rousseau E, et al. Trisomy 19 ependymoma, a newly recognized genetico-histological association, including clear cell ependymoma. Mol Cancer. 2007; 6:47. [PubMed: 17626628]
29. Phillips HS, et al. Molecular subclasses of high-grade glioma predict prognosis, delineate a pattern of disease progression, and resemble stages in neurogenesis. Cancer Cell. 2006; 9:157–173. [PubMed: 16530701]
30. Thompson MC, et al. Genomics identifies medulloblastoma subgroups that are enriched for specific genetic alterations. J Clin Oncol. 2006; 24:1924–1931. Epub 2006 Mar 1927. [PubMed: 16567768]

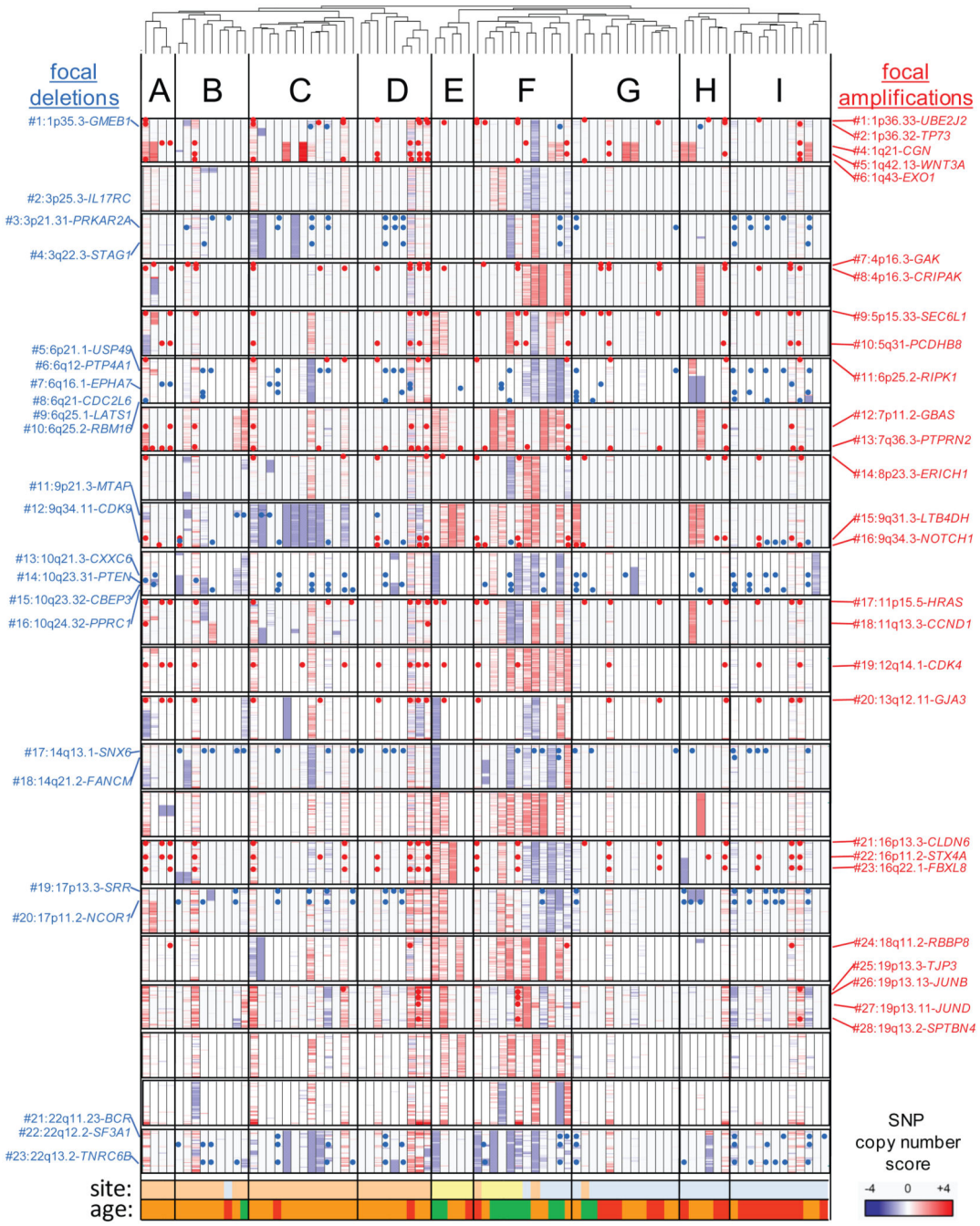

Figure 1. The ependymoma genome

Dendrogram at top segregates 83 human ependymomas into nine subgroups (A to I) according to mRNA expression profiles. Clusters were validated by two distinct methods that confirmed agreement for location (Rand index=0.93, P<0.0001) and subgroup (Rand index=0.87, P<0.0001). Heatmap below reports in columns for each case chromosomal gains (red) and losses (blue). Each row represents a chromosome. Red ‘dots’ report focal amplifications (details right), blue ‘dots’ focal deletions (details left). Details are reported in

the Supplemental Gene Cards. Site: supratentorial (pink), posterior fossa (blue), spine (yellow). Age: patients <3 years (red), 3–21 years (orange), >21 years (green).

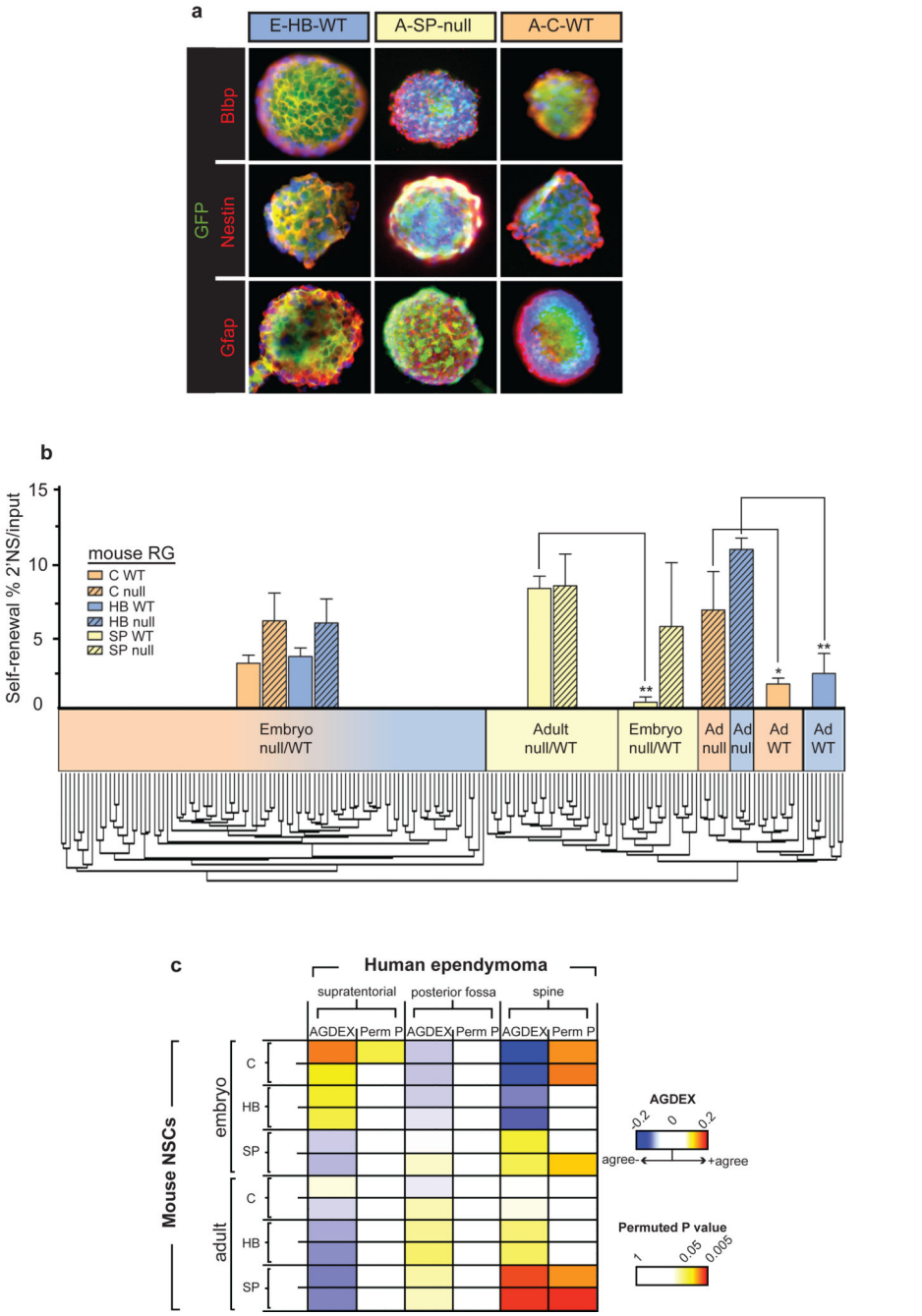

Figure 2. Regionally, developmentally and genetically discrete NSCs match subgroups of human ependymoma

a. Co-immunofluorescence of neurospheres generated by NSC from the cerebrum (C), hindbrain (HB) and spine (SP) of embryonic (E) and adult (A) *Ink4a/Arf* null or WT *Blbp-eGFP* mice. **b**. Graph of percentage of multi-potent daughter neurospheres formed from each NSC type. Dendrogram segregates 177 NSC isolates into subgroups according to mRNA expression. **c**. Heatmap of transcriptomic (AGDEX, 14,261 orthologs) agreement between mouse NSCs and human supratentorial, posterior fossa and spinal ependymomas.

NB. Supratentorial ependymomas match only embryonic cerebral *Ink4a/Arf* null NSCs; spinal ependymomas match mouse adult spinal NSCs.

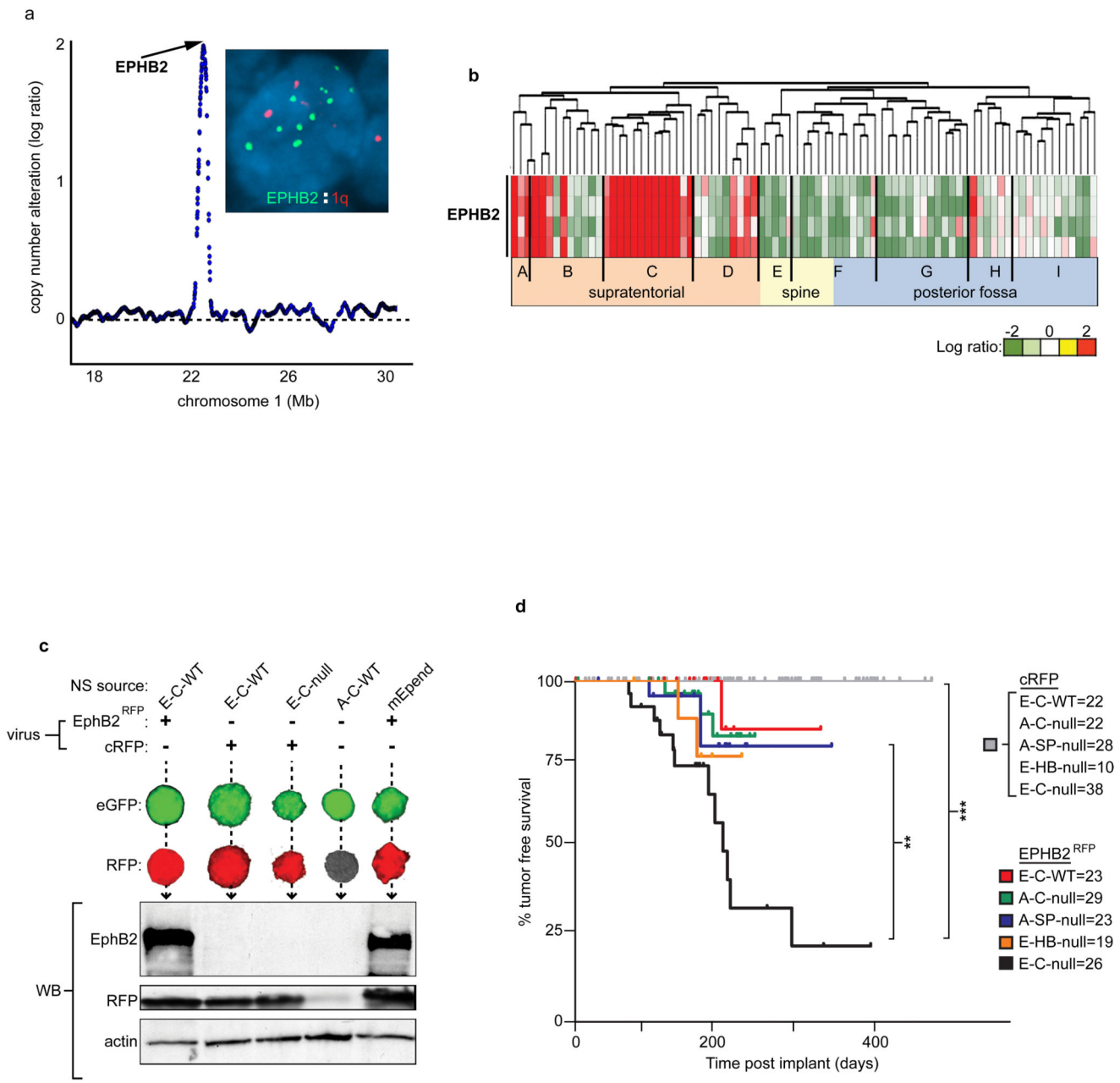

Figure 3. *EPHB2* is an ependymoma oncogene that selectively transforms embryonic cerebral *Ink4a/Arf*$^{-/-}$ NSCs

a. SNP array profile infers focal *EPHB2* amplification in human supratentorial ependymoma, validated by FISH analysis (inset) of the *EPHB2* locus. **b**. Profiles of *EPHB2* mRNA expression in the human ependymomas shown in Figure 1. **c**. eGFP/RFP co-immunofluorescence (top) and EphB2, RFP western blot analysis (below), of eGFP^{+} NSCs transduced with *Ephb2* (*Ephb2*^{RFP}) or control (cRFP) virus. **d**. Tumor free survival of mice implanted with *Ephb2*^{RFP} or control transduced cells. Numbers next to each NSC type indicate the number of implanted mice (**, P<0.005; ***, P<0.0005, Log Rank Test).

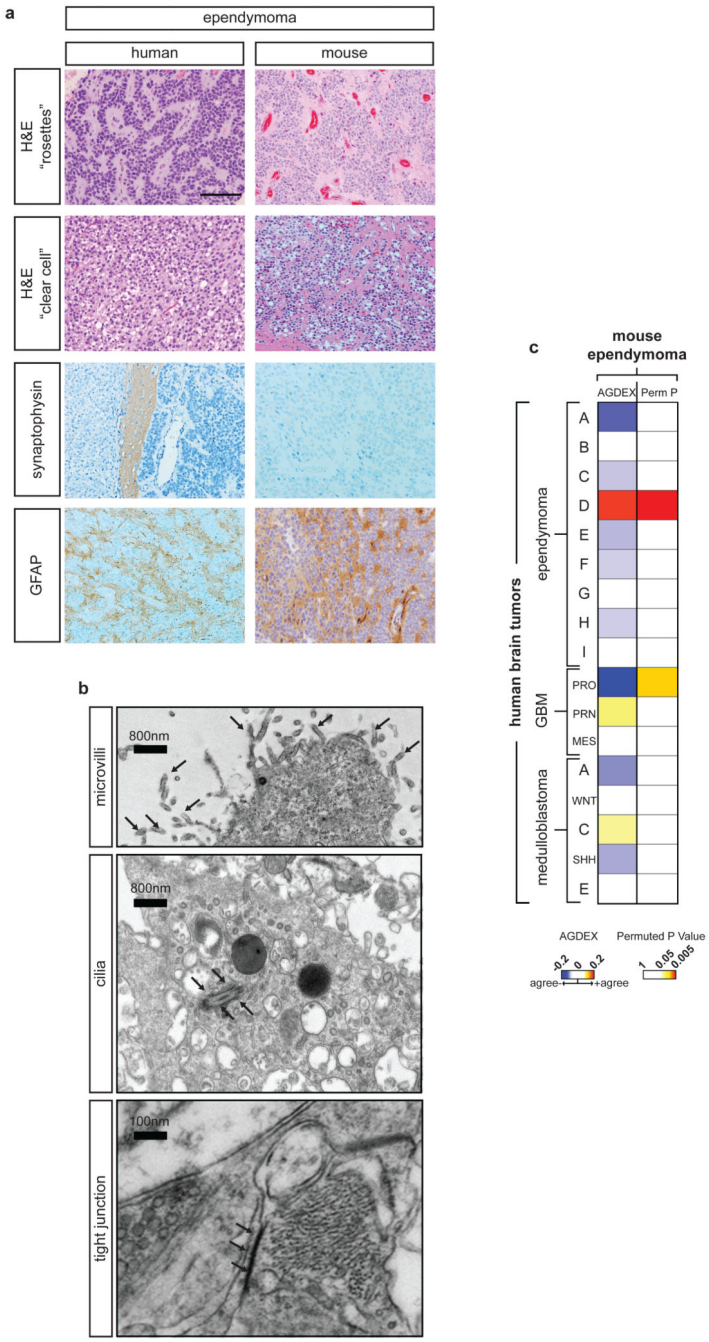

Figure 4. *Ephb2*-driven mouse ependymomas model human subgroup 'D' tumors

a. Comparative histology of a representative human cerebral (left) and *Ephb2*-driven mouse (right) ependymoma including the neuronal marker synaptophysin and glial marker glial fibrillary acidic protein (GFAP). Scale bar=100μm, all panels. **(b)** Electron micrographs of *EphB2*-driven mouse ependymomas showing three ultrastructural hallmarks of human ependymoma. **(c)** Heatmap reporting the transcriptomic agreement (AGDEX) and corresponding permuted p-value in comparisons between *EphB2*-driven mouse

ependymoma and 18 molecular subtypes of human brain tumor. **NB**. Mouse ependymomas matched only human subgroup D ependymomas.